Sensors and Materials, Vol. 28, No. 5 (2016) 523–530
MYU Tokyo

S & M 1205

Study of Structural and Optical Properties of ZnO Thin Films Produced by Sol–Gel Methods

Huai-Shan Chin, Long-Sun Chao,* and Kuo-Sheng Kao[1]

Department of Engineering Science, National Cheng Kung University,
No. 1 University Road, Tainan 70101, Taiwan
[1]Department of Computer and Communication, Shu-Te University,
No. 59 Hengshan Road, Kaohsiung 82445, Taiwan

(Received August 31, 2015; accepted March 4, 2016)

Keywords: ZnO thin film, electroluminescence, photoluminescence, sol–gel, chemical configuration analysis

This study adopted sol–gel and spin-coating methods for fabricating ZnO thin films on Pt/Ti/Si substrates. Each layer is carbonized at a low temperature and finally sintered at a high temperature for spin-coating. The luminescent characteristics of ZnO films were investigated using photoluminescence (PL). The crystal structures of the films were determined by X-ray diffraction (XRD), scanning electron microscopy (SEM), and transmission electron microscopy (TEM). X-ray photoelectron spectroscopy (XPS) was used to analyze the chemical states of ZnO thin films. The platinum and aluminum layers were deposited as top and bottom electrodes, respectively. The sandwich structure of electroluminescence (EL) elements was fabricated and its conductivity was measured. The SEM images showed that the surface roughness of the thin films and the grain size improved as the thickness of the films increased. These results were verified by XRD patterns in which the peak intensities of the ZnO (002) C preferred orientation increased as the thin films thickened. In addition, enhanced crystallinities increased the ultraviolet (UV) radiation intensities of the ZnO thin films. Moreover, only UV radiation excited through the intrinsic band gap was observed in the PL spectra, and no visible light was produced by the luminescence mechanisms of defects. Moreover, the chemical configuration analysis of the thin films revealed that the proportions of O–Zn bonding and Vo increased and decreased respectively as the number of spin-coated layers increased. These results indicate that increased thin film thickness reduces thin film internal defects and improves the ZnO structure. Regarding the EL measurements of the EL elements, at a ZnO film thickness of 530 nm, the threshold and alternating-current working voltages were 25 and 33 V, respectively.

1. Introduction

As computer, communication, and network technologies have rapidly developed, people's demands regarding display technologies have increased. In addition to fast and convenient communication devices, users prefer instant and convenient display terminals with excellent visibility. In recent years, the development and improvement of displays have continued to progress toward more compact dimensions. Thus, display development has led to active research

*Corresponding author: e-mail: lschao@hflow.es.ncku.edu.tw

ISSN 0914-4935 © MYU K.K.

on flatness, portability, and space- and power-saving qualities. Consequently, traditional cathode-ray tubes have gradually been replaced by various flat-panel displays (FPDs), which have been rapidly developed to become the mainstream of the new display generation.

Currently, FPDs comprise liquid-crystal displays, organic light-emitting diode displays, plasma display panels, field-emission displays, and electroluminescence (EL) displays. Among these technologies, the EL element is an active display featuring advantageous properties such as the entire plane, full viewing angle, all solid state, high-speed response, long operating life, favorable adaptation, low power consumption, low temperature (high luminescence efficiency), soft and uniform lighting, soft and flexible display, and compact dimensions. Thus, this type of display has received considerable attention from research units in recent years and is a display product with tremendous potential. Based on the various drive voltages and semiconductor material types, EL can roughly be divided into four categories: direct-current powder, direct-current thin-film, alternating-current powder, and alternating-current thin-film EL.

Among the currently developed high-efficiency, low-voltage color fluorescent powders, ZnO:Zn, Gd_2O_2S:Tb, and ZnCdS:(Cu, Al) are among the materials that have received the most attention. ZnO thin films are a type of direct-gap III–V metal-oxide semiconductor that features a hexagonal close-packed wurtzite structure. The high melting point (1975 °C), stable chemical properties, self-excited luminescence, and intense ultraviolet (UV) radiation make ZnO a focus of research.

Currently, ZnO thin films can be fabricated using spray pyrolysis,[1] metal organic chemical vapor deposition,[2,3] electron beam evaporation,[4] radio frequency sputtering,[5–9] thermal oxidation,[10] pulsed laser deposition,[11] molecular beam epitaxy,[12,13] and sol–gel[14–16] methods. Among these methods, the sol–gel method uses a nonvacuum coating process that features the advantages of simple fabrication and low equipment cost and thus exhibits extremely high market application potential. This study applied the sol–gel method involving spin-coating techniques immediately followed by rapid thermal annealing for fabricating ZnO thin films. Subsequently, a series of physical investigations and analyses of optoelectronic properties were performed on the thin films.

2. Materials and Methods

2.1 Experimental fabrication process

<u>Substrate fabrication</u>: This study used a p-type (boron doped) 5–8 Ωcm silicon wafer with a crystal direction of (100) as the substrate. A layer of platinum (Pt) was sputtered onto the upper surface as the base electrode for the EL elements. However, Pt exhibited low adhesion to the silicon substrate; thus, a layer of titanium (Ti) was preliminarily deposited to facilitate the adhesion of Pt. Table 1 shows the specific Pt and Ti deposition conditions.

<u>Fabricating ZnO thin films by spin-coating</u>: This study adopted a two-stage spin-coating method (the first stage was spun at 1000 rpm for 10 s, and the second stage was spun at 2000 rpm for 20 s) to fabricate the ZnO thin films. The purpose of the first stage was to distribute the coating solution evenly at a low rotation speed. A higher rotation speed was then used at the second stage to remove the excess solution and enhance coating uniformity. First, the Pt/Ti/Si substrate was processed using O_2 plasma. Then, a thermal resistant tape was used to preserve surface areas of 0.5 × 2 cm^2 on the substrate electrode before placing the substrate on the vacuum suction seat of the spin (photoresist) coater. A syringe was used to extract the ZnO solution, which was uniformly dropped over the Pt/Ti/Si substrate for spin-coating (Fig. 1).

Table 1
Pt and Ti deposition conditions.

Materials	Ti	Pt
Substrate	Si	Ti/Si
Working pressure	3×10^{-3} Torr	1×10^{-3} Torr
DC power	75 W	175 W
Ar flow	7 sccm	7 sccm
Thickness	12 nm	100 nm

Table 2
SiO_2 deposition conditions.

Materials	SiO_2
Substrate	Si
Pressure	1000 mTorr
RF power	25 W
N_2O flow	710 sccm
SiH_4 flow	25 sccm
Thickness	100 nm

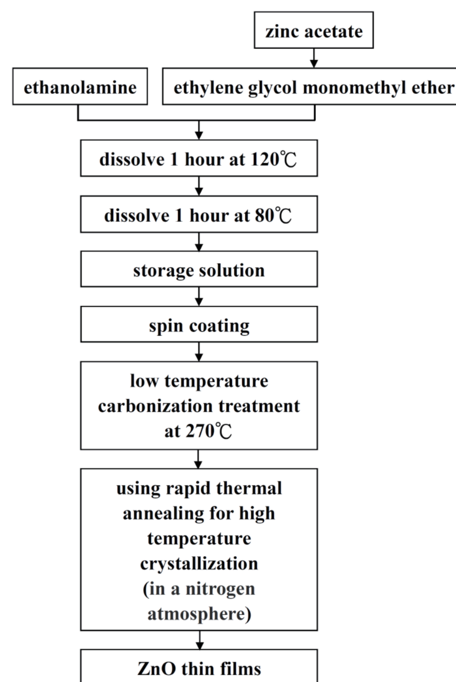

Fig. 1. The preparation of the ZnO solutions.

Heat treatment process: After the thin-film fabrication process was completed, the sample was immediately carbonized at a low temperature to remove the organic solvents in the thin films and convert the metal-organic compound into an inorganic thin film. By using low-temperature carbonization treatment, most thin films retain their amorphous structures. Additional heat treatment is required to form crystalline structures to promote thin-film crystallization and crystal growth. This experiment involved rapid thermal annealing as a high temperature crystallization heat treatment. The annealing temperature was 900 °C and was maintained for 3 min.

EL element fabrication: The initial step in the fabrication of the elements was depositing silicon dioxide (SiO_2) as a dielectric layer on the ZnO-coated Pt/Ti/Si substrate to prevent current leakage from influencing the luminescence properties during measurements. Table 2 shows the SiO_2 deposition conditions. Subsequently, 100-nm aluminium (Al) thin films were deposited on the SiO_2 layers as the top electrode to complete the EL prototype element. Figure 2 shows the complete structure of the elements.

2.2 Measurement and analyses

This study used a field emission scanning electron microscope (FE-SEM) to observe the thin-film surface and cross-sectional crystalline morphology under various fabrication conditions. X-ray diffraction (XRD) was used to examine variations in thin-film crystalline structure produced using different experimental parameters, photoluminescence (PL) was used to measure radioactive emission properties of the samples, X-ray photoelectron spectroscopy (XPS) multiplex was used to analyze chemical configurations within the thin films, and EL measurements were performed to investigate the threshold and working voltages of the elements.

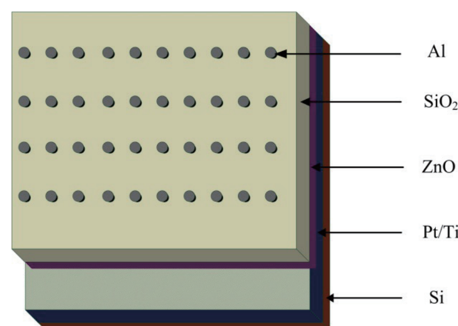

Fig. 2. (Color online) Complete structure of the elements.

3. Results and Discussion

3.1 Thin film structure and crystallinity analysis

Figure 3 shows the SEM surface and cross-section topographical images of the ZnO thin films. The surface images clearly showed that the surface of the 225-nm thin film consisted of individual pebble-like structures. The surface exhibited small grains and large spacings and thus featured a relatively high surface roughness. When the thickness was increased to 433 nm, minor pores remained on the thin-film surface, but grain size increased and spacing decreased; thus, the surface was comparatively smooth. The surface of the 530-nm thin film exhibited apparent grain growth and decreased grain spacing distances that nearly eliminated surface porosities and was thus extremely smooth. In addition, the XRD results (Fig. 4) verified that the preferred ZnO (002) C axis peak value increased as the number of spin coats increased. The grain size of the ZnO thin films was determined by the recrystallization temperature. With appropriate control of annealing temperature, the ZnO thin films could attain an excellent level of crystallization. In our study, under an annealing temperature of 900 °C, the grains enlarge and the grain boundaries reduce owing to sufficient processing time. At the same time, a process of sufficient duration would lead to increased thickness with an increasing crystallinity closer to the bulk property. Furthermore, a process of sufficient duration would lead to increasing thickness with an increasing grain size. An increasing grain size affects the full width at half maximum (FWHM) value.

3.2 PL property measurement

Figure 5 shows PL spectra of the ZnO thin films. The spectra clearly show that, except for a UV radiation peak at 380 nm, no visible light radiation was observed. As the thickness of the film and grain size increased, the intensity of UV radiation gradually increased. According to Ref. 17, ZnO can simultaneously exhibit visible and UV luminescence. UV radiation is a type of intrinsic band gap luminescence, whereas radiation from the remaining visible spectrum is generally considered to be associated with mechanisms involving defects within the thin film, specifically a form of luminescence produced when F-centers are subjected to impacts facilitated by an increase in pressure (internal defects of the thin film). However, no radiation from the visible spectrum was observed in the PL spectra, indicating that the ZnO thin films fabricated in this experiment exhibited excellent crystallinity and relatively few defects.

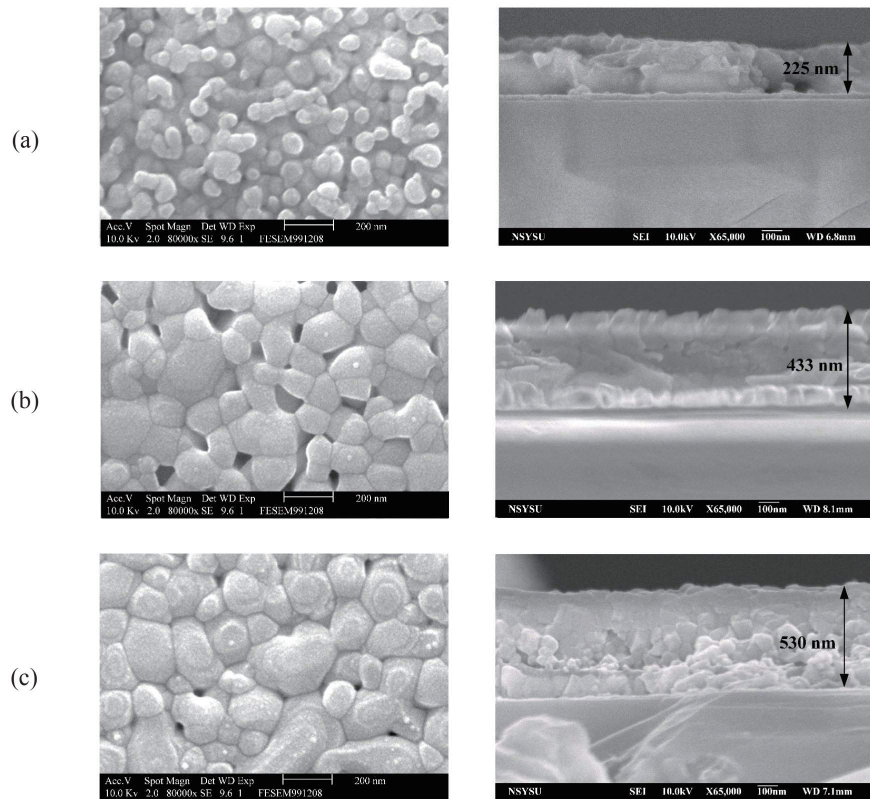

Fig. 3. SEM surface and cross-section topographical images of various layers of ZnO thin films: (a) four, (b) eight, and (c) twelve layers.

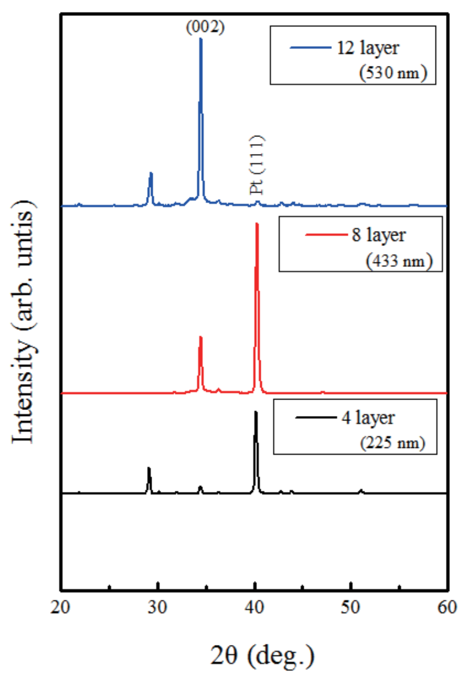

Fig. 4. (Color online) XRD patterns of ZnO thin films.

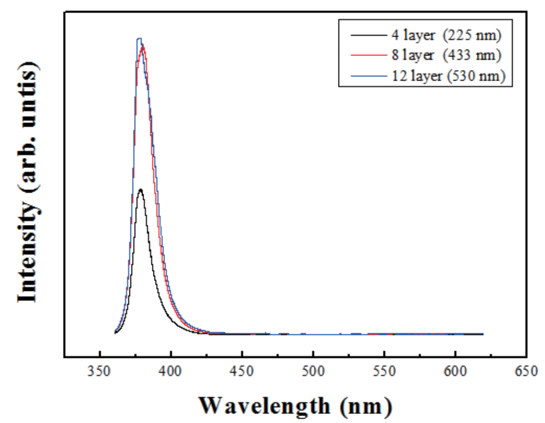

Fig. 5. (Color online) PL spectra of ZnO thin films.

3.3 Analysis of chemical configuration of thin films

To investigate the relationship between the luminescence properties of the ZnO thin films and the chemical bonding within the thin-film compositions, the XPS multiplex results were analyzed. The multiplex provides a slow scan of specific shells of specific elements, and the peaks generated can be used to calculate the proportion of specific bonds present in the material. This study focused on calculation of the O 1s multiplex spectrum. Figure 6 presents the results of the Gaussian fit of various ZnO thicknesses obtained using the multiplex.

Oxygen demonstrates various forms of bonding which exhibit complex bond energies. In ZnO, O 1s primarily comprises three bond energy positions, which are described as follows:

(1) 1s (530.15 ± 0.15 eV): This is the bond energy when O^{2-} and Zn^{2+} ions are arranged and bonded in the hexagonal wurtzite structure.[18]

(2) 1s (531.25 ± 0.2 eV): This is the bond energy when O^{2-} ions are insufficient in the ZnO matrix, causing oxygen vacancies (V_o),[18,19] or the bond energy characterized by O^{2-} and Al^{3+} ions.

(3) 1s (532.65 ± 0.15 eV): This is the bond energy of loosely bound oxygen on the thin-film surface bonding with other specific compounds (i.e., CO_2, H_2O, O_2, and the oxidation layer of the silicon substrate, which is SiO_2).

In this study, the three O 1s bond energies of various thicknesses of ZnO thin films were plotted as statistical charts (Fig. 7) based on relative proportions. The figure shows that the proportion

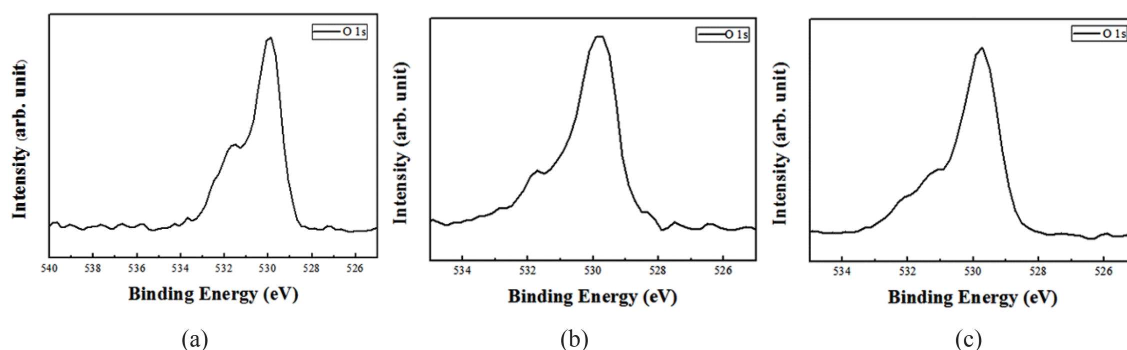

Fig. 6. Multiplex results for various thicknesses of ZnO thin films: (a) 225, (b) 433, and (c) 530 nm.

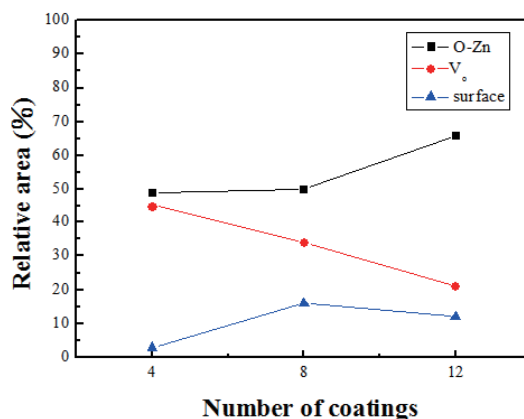

Fig. 7. (Color online) O 1s statistical charts for various thicknesses of ZnO thin films.

of O–Zn 1s bonding increased as the film thickness increased from 48 to 66%. An increasing proportion of O–Zn bonding indicated a more complete Zn oxidation within the thin film, which produced improved ZnO structures. The V_o bond ratio decreased from 45 to 21%, indicating reduced internal thin-film defects and enhanced thin-film crystallinity. Surface bond energies were maintained at less than 20%, which exerted negligible influence on thin-film properties.

3.4 EL measurement and analysis

The ZnO thin films were ultimately fabricated into EL elements. The structure of the EL elements is shown in Fig. 2. In this structure, Pt was the base electrode, ZnO was the luminescent material (fluorescent layer), SiO_2 was the dielectric layer, and Al was the top electrode.

To discuss the *I–V* curve of the ZnO thin films, the devices were denoted as A (with the thinnest ZnO films) and B (with the thickest ZnO films). Devices A and B are designed and fabricated with the same geometry, and the thicknesses of the ZnO thin films were 225 nm and 530 nm, respectively. Moreover, to conform closely to the operating conditions of the alternating-current thin-film EL, an alternating current was applied to the EL elements at a frequency of 1 kHz. As shown in Fig. 8, at device A, the threshold and alternating-current working voltages were 23 and 30 V, respectively. As shown in Fig. 9, at device B, the threshold and alternating-current working voltages were 25 and 33 V, respectively.

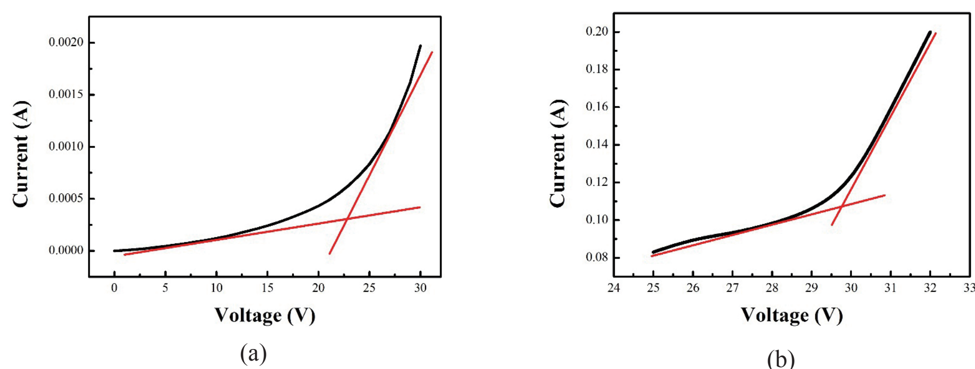

Fig. 8. (Color online) (a) Threshold and (b) alternating-current working voltage curves of device A.

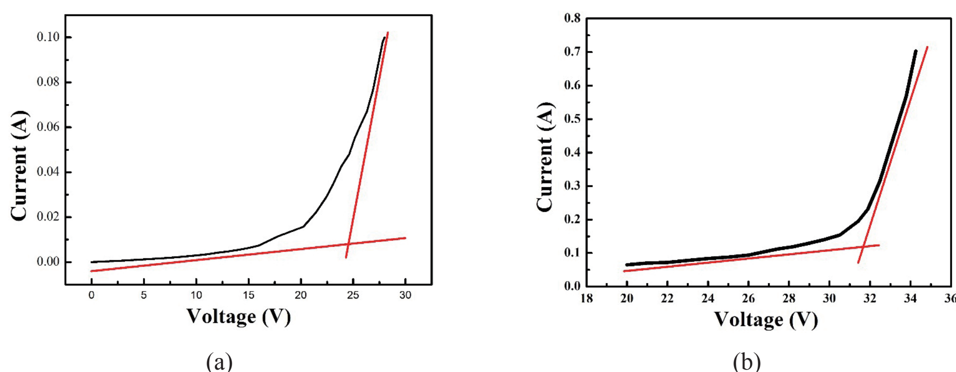

Fig. 9. (Color online) (a) Threshold and (b) alternating-current working voltage curves of device B.

4. Conclusion

This study adopted sol–gel and spin-coating methods to fabricate ZnO thin films on Pt/Ti/Si substrates. By adjusting the number of spin-coated layers, the influence of various film thicknesses and crystallinities on the luminescence properties of ZnO was investigated. The SEM images showed that the thin-film surface roughness and grain size improved as the film thickness increased. These results were verified in XRD patterns in which the ZnO (002) C preferred orientation peak intensities increased as the thin films thickened. In addition, enhanced crystallinity increased the UV radiation intensities of the ZnO thin films. Moreover, only UV radiation excited through the intrinsic band gap was observed in the PL spectra, and no visible light was produced through the luminescence mechanisms associated with defects. Moreover, the analysis of the chemical configuration of the thin films revealed that the proportions of O–Zn bonding and V_o increased and decreased, respectively, as the number of spin-coated layers increased. These results indicate that increased film thickness reduces thin-film internal defects and improves the ZnO structure.

References

1 K. H. Yoon and J. Y. Cho: Mater. Res. Bull. **35** (2000) 39.
2 Z. Fu, B. Lin, and J. Zu: Thin Solid Films **402** (2002) 302.
3 J. Ye, S. Gu, S. Zhu, T. Chen, L. Hu, F. Qin, R. Zhang, Y. Shi, and Y. Zheng: J. Cryst. Growth **243** (2002) 151.
4 Y. Nakanishi, A. Miyake, H. Kominami, T. Aoki, Y. Hatanaka, and G. Shimaoka: Appl. Surf. Sci. **142** (1999) 233.
5 X. H. Li, A. P. Huang, M. K. Zhu, Sh. L. Xu, J. Chen, H. M. Wang, B. Wang, and H. Yan: Mater. Lett. **75** (2003) 4655.
6 W. Water and S. Y. Chu: Mater. Lett. **55** (2002) 67.
7 Y. H. Liu, S. J. Young, L. W. Ji, T. H. Meen, C. H. Hsiao, C. S. Huang, and S. J. Chang: IEEE Trans. Eelectron Devices **61** (2014) 1541.
8 C. Z. Wu, L. W. Ji, C. H. Liu, S. M. Peng, S. J. Young, K. T. Lam, and C. J. Huang: J. Vac. Sci. Technol. A **29** (2011) 03A118.
9 S. J. Young: IEEE Sens. J. **11** (2011) 1129.
10 Y. G. Wang, S. P. Lau, X. H. Zhang, H. W. Lee, S. F. Yu, B. K. Tay, and H. H. Hng: Chem. Phys. Lett. **375** (2003) 113.
11 S. H. Bae, S. Y. Lee, H. Y. Kim, and S. Im: Appl. Surf. Sci. **168** (2000) 332.
12 K. Sakurai, M. Kanehiro, K. Nakahara, T. Tanabe, and S. Fujita: J. Cryst. Growth **209** (2000) 522.
13 S. J. Young, L. W. Ji, S. J. Chang, and Y. K. Su: J. Cryst. Growth **293** (2006) 43.
14 D. G. Baik and S. M. Cho: Thin Solid Films **354** (1999) 227.
15 P. Sagar, P. K. Shishodia, R. M. Mehra, H. Okada, A. Wakahara, and A. Yoshida: J. Lumin. **126** (2007) 800.
16 K. J. Chen, F. Y. Hung, S. J. Chang, and S. J. Young: Mater. Trans., JIM **50** (2009) 922.
17 B. Lin, Z. Fu, Y. Jia, and G. Liao: J. Electrochem. Soc. **148** (2001) G110.
18 M. Chen, X. Wang, and Y. H. Yu: Appl. Surf. Sci. **158** (2000) 134.
19 L. Yi, Y. Hou, H. Zhao, D. He, Z. Xu, Y. Wang, and X. Xu: Displays **21** (2000) 147.